

The intensity distribution and thermal stability of InnoSlab laser

Ning Wang (王宁), Peng Shi (石鹏), and Yutian Lu (陆雨田)

Shanghai Institute of Optic and Fine Mechanics, Chinese Academy of Sciences, Shanghai 201800

Received August 30, 2004

Partially end-pumped slab laser is an innovative solid state laser, namely InnoSlab. Combining the hybrid resonator with partially end-pumping, the output power can be scaled with high beam quality. In this paper, the output intensity distributions are simulated by coordinate transformation fast Fourier transform (FFT) algorithm, comparing the thermal lens influence. As the simulated curves showed, the output mode is still good when the thermal lens effect is strong, indicating the good thermal stability of InnoSlab laser. Such a new kind of laser can be designed and optimized on the base of this simulation.

OCIS codes: 140.0140, 140.3410, 140.3580.

High output power and high beam quality are two contrary characteristics for the conventional solid state laser. A novel solid state laser, partially end-pumped slab laser, namely InnoSlab, is invented by K. Du *et al.*^[1], combining the hybrid resonator with partially end-pumping, the output power can be scaled at high beam quality^[2,3]. In *Q*-switching mode, high repetition frequency and narrow pulse width are obtained with high power and high beam quality^[4,5], keeping the compact configuration simultaneously. But the analyzing for InnoSlab is very little and simple^[6] yet. Fast Fourier transform (FFT) algorithm is a convenient method for simulating the intensity distribution of resonator. Because the hybrid resonator is off-axial and non-axial symmetric, the usual FFT algorithm can not be used, due to aliasing in the Fourier spectrum^[7]. In this paper, on the base of Sziklas's and Siegman's wave function coordinate transformation theory^[7], the output intensity distributions of off-axial hybrid resonator are simulated, which indicates good thermal stability of InnoSlab laser.

In this new design, the volume pumped by a line-shaped beam has a rectangular cross section, which underfills the slab (partially end-pumped) and forms a gain sheet in the central portion of the slab. Unlike the conventional slab laser, the gain has the same cross section as the slab. The resonator consists of two highly reflecting cylindrical mirrors, as shown in Fig. 1. One is concave and the other is convex. Their cylindrical axes are in the vertical plane. The curvature radii of the mirrors and the distance between the mirrors are defined in such a way that the foci of the mirrors are at the same position. Therefore, in the horizontal plane a confocal

unstable positive-branch cavity is formed by the concave and convex surfaces of the mirrors. Different from unstable resonator of negative-branch with the same resonator length, unstable resonator of positive-branch has no intracavity focus and the divergence angle inside the resonator is lower. Those made them more favourable for *Q*-switching operation. In the vertical plane, a flat-flat resonator is configured. The slab crystal is put inside the cavity with large faces perpendicular to the cylindrical axes of the mirrors, and a side surface matches the lineshaped pumping beam. The large faces of crystal are cooled well.

FFT algorithm is an efficient method for simulating the intensity distribution of resonator. Compared with the usual diffraction integral numerical iterative algorithm, the primary merit of FFT algorithm is saving time greatly^[7]. The FFT process, straightforwardly applied, requires that the input and output wave functions are sampled on the same equally spaced transverse grid. This means that for a diverging optical wave, which is characteristic of the expanding beam portion of a positive-branch confocal unstable optical resonator, the usual FFT algorithm can not be used, due to aliasing in the Fourier spectrum^[7]. This difficulty can be remedied by coordinate transformation FFT algorithm based on Gaussian beam theory.

As the Sziklas's and Siegman's thesis showed, the Fourier transforming wave function satisfies paraxial wave equation,

$$\left(\frac{\partial^2}{\partial x^2} + \frac{\partial^2}{\partial y^2} + 2ik\frac{\partial}{\partial z}\right)\psi(x, y, z) = 0. \quad (1)$$

The equation is still satisfied if the wave function changes as $\psi(x, y, z) = \frac{1}{z} \exp(i\frac{kz^2}{2z})F(x', y', z')$. Where $r^2 = x^2 + y^2$, $x' = \frac{\alpha x}{z}$, $y' = \frac{\alpha y}{z}$, $z' = \alpha^2(\frac{1}{z_0} - \frac{1}{z})$, and α and z_0 are arbitrary constant. The new wave function $F(x', y', z')$ still satisfies the paraxial equation. Utilizing this smart coordinate transformation, the divergence of initial wave equation is corrected. If $\alpha = z_0 + L$, the coordinate transformation at beginning plane ($z = z_0$) is $x' = Mx$, $y' = My$, $z' = 0$. Rightly choosing the value of z_0 , the coordinate transformation will satisfy the expanding propagation method^[7]. The propagation is equal to col-

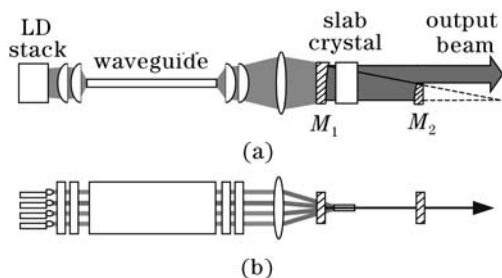


Fig. 1. Experimental setup. (a) Horizontal direction and (b) vertical direction.

limited propagation in new coordinate system,

$$M = \frac{z_0 + L}{z_0},$$

where L is transforming distance, M is magnification ratio, and $z_0 = \frac{L}{M-1}$. The divergence wave transformed from the little plane ($z = z_0$) to the large size plane ($z = z_0 + L$). So at the large end plane $x' = x$, $y' = y$, $z' = ML$. If the initial wave function is Ψ_0 , and the area is divided with $N \times N$ sampling points, at the initial plane, the wave function transformation (equal to passing through a lens with focus z_0) is

$$F_0 = z_0 \exp(-i \frac{kr^2}{2z_0}) \Psi_0. \quad (2)$$

By coordinate transformation and wave function transformation, the usual FFT algorithm can be used. The transforming distance is $L' = ML$. The wave function transforming to large end plane is

$$F_1 = F^{-1} \{ F(F_0) e^{-i\pi\lambda L' (f_{x'}^2 + f_{y'}^2)} \}. \quad (3)$$

By wave function transformation, it is

$$\Psi_1 = \frac{1}{z_0 + L} \exp(i \frac{kr^2}{2(z_0 + L)}) F_1. \quad (4)$$

The upper transformation is free transforming for diverging spherical wave function Ψ_0 . For hybrid resonator, the coordinate transformation FFT algorithm is only used in unstable direction. So the round-trip between two resonator mirrors is shown in Fig. 2. When the wave has experienced round-trip many times, the phase distribution and amplitude distribution should be reappearing. For simplicity, unconsidering the laser media gain, the wave function transformation equation is

$$u_1(x', y') = F^{-1} \{ F \{ z_0 \exp(-i \frac{ky^2}{2z_0}) \Psi_0 \cdot P_1 \cdot e^{i\pi\lambda(Lf_{x'}^2 + MLf_{y'}^2)} \}, \quad (5)$$

$$u_2(x', y') = F^{-1} \{ F \{ \frac{1}{z_0 + L} \exp(i \frac{ky'^2}{2(z_0 + L)}) u_1 \cdot P_2 \cdot \exp(-i \frac{ky'^2}{2f_1}) \cdot e^{i\pi\lambda L(f_{x'}^2 + f_{y'}^2)} \}, \quad (6)$$

where $u_1(x', y')$ and $u_2(x', y')$ are the wave function at cylindrical mirror M_1 and cylindrical mirror M_2 , P_1 and P_2 are diaphragm functions at M_1 and M_2 , $\Psi_0 = A \exp(-i \frac{ky^2}{2f_2})$, A is constant. For the confocal unstable positive-branch cavity, $f_2 = -z_0$, $f_1 = z_0 + L$.

According to Ref. [6], front cylindrical mirror M_1 , radii of curvature $R = 500$ mm; back cylindrical mirror, radii of curvature $R = -350$ mm. Unconsidering the thermal lens effect of the slab crystal, the output near-field intensity distribution is shown in Fig. 3. Because of the line shaped pumping beam and good cooling at two large planes, the thermal conduction is quasi-one-dimensional, which causes the temperature gradient in the direction

perpendicular to the pumping line. Therefore, there is thermal-lens only in stable resonator direction. So the thermal lens is equal to a cylindrical lens. Let $f = 120$ mm^[6], with the distance 10 mm to cylindrical mirror M_1 . The output near-field and far-field intensity distributions are also simulated as shown in Figs. 4 and 5.

Obviously, the intensity distribution is Gaussian distribution in x -direction (the stable direction). In fact, the stability is determined by thermal lens. But in y -direction (the unstable direction), the intensity distribution is modulated because of the hard-edge diffraction^[8]. The beamwidth along the unstable direction is bigger than that along the stable direction. The different beam shapes along two directions are related to the cylindrical mirror resonator. The focusing effect of the thermal lens makes beamwidth smaller in the stable direction. Because of the quasi-one-dimensional thermal distribution in slab crystal, the thermal lens effect mainly affects the intensity distribution in x -direction. When

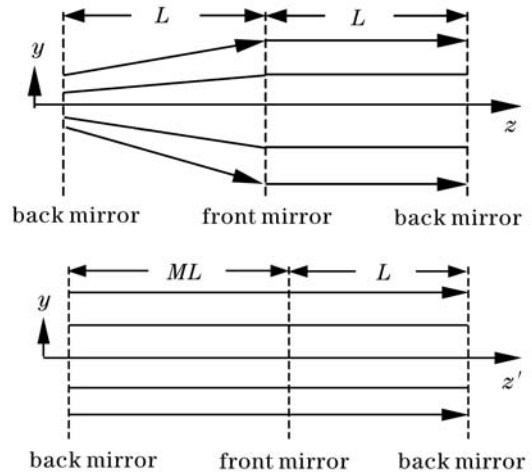


Fig. 2. Schemes of round beam (unstable resonator direction) without (a) and with coordinate change (b).

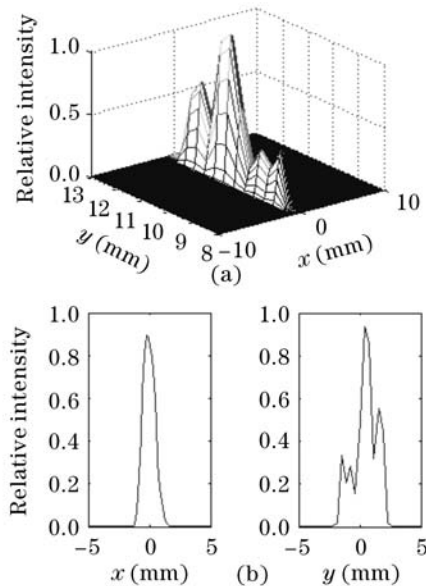


Fig. 3. (a) Three- and (b) two-dimensional distribution of the output intensity.

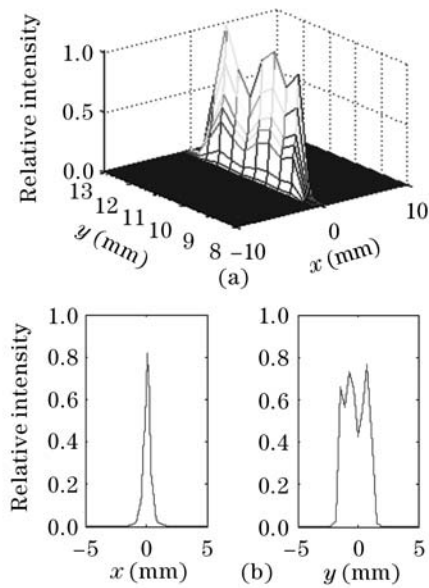


Fig. 4. (a) Three- and (b) two-dimensional distribution of the output intensity considering thermal lens.

$f = 120$ mm, the thermal lens effect is very strong. But the output mode is still good, as shown in Figs. 4 and 5. This indicated the good thermal stability of InnoSlab laser. So the high power output can be obtained at high beam quality by hybrid resonator. Certainly, the homogeneous lineshaped pumping beam and good cooling at two large faces must be satisfied.

In fact, more than one hundred watts power output with near diffractive-limit has been obtained by P. Shi *et al.*^[2]. The measured near-field intensity distribution curve^[2] is shown in Fig. 6. Good far-field intensity distribution has also been obtained by K. Du *et al.*^[2,3] as shown in Fig. 7. The resonator parameters in simulation are the same as those in experiments. Obviously, the simulated curves resemble the measured curves well. The curve is Gaussian along stable direction, and the distribution is modulated along unstable direction. The modulation in the distribution curve of unstable direction is obvious. Because the measured points are more than sampling points in simulation, the modulation in simulated curve is not severe as measured curve, but the trend is uniform. The beamwidth along unstable direction

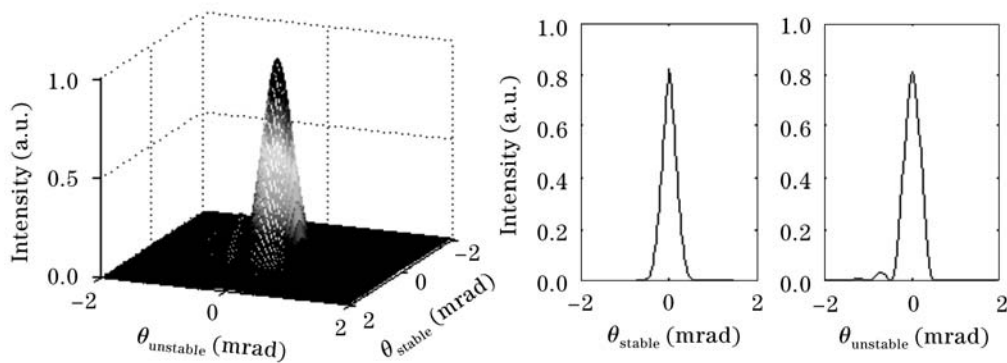


Fig. 5. Simulated intensity distribution in the far-field with side lobes.

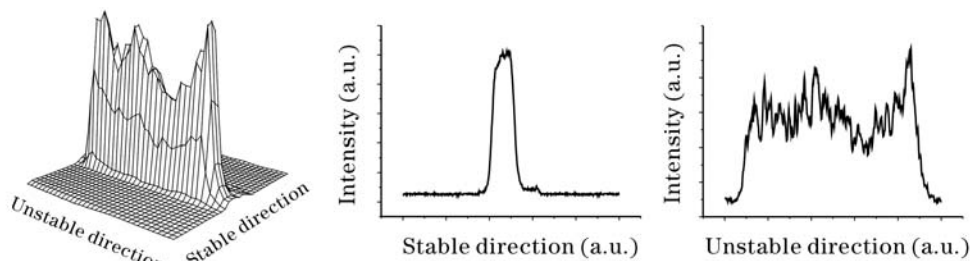


Fig. 6. Intensity distribution of the output beam.

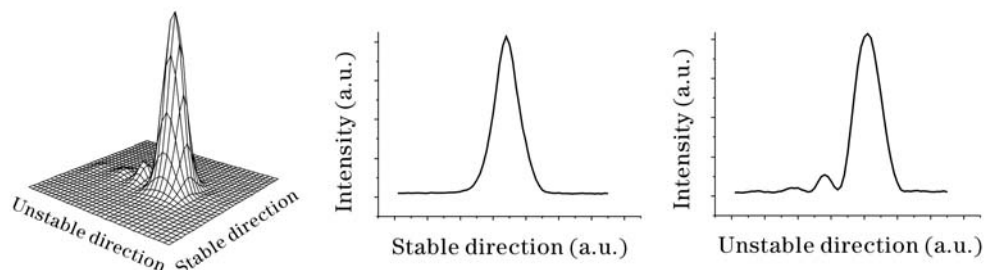


Fig. 7. Intensity distribution in the far-field with side lobes.

is bigger than that along stable direction too. So the simulated results by coordinate transformation FFT algorithm is satisfying.

In this paper, the output near-field and far-field intensity distributions are simulated by coordinate transformation FFT algorithm, comparing the thermal lens influence. The simulated curves well resemble the measured curves in experiments. The difference between stable direction and unstable direction is also discussed. As the simulated curves showed, the output mode is still good when the thermal lens effect is strong, indicating the good thermal stability of InnoSlab laser. This implies that the output power can be scaled at high beam quality. The theoretic simulations are important for understanding this slab laser. This laser can be designed and optimized on the base of this simulation.

N. Wang's e-mail address is qfwangning@163.com.

References

1. K. Du, N. Wu, J. Xu, J. Giesekus, P. Loosen, and R. Poprawe, *Opt. Lett.* **23**, 370 (1998).
2. P. Shi, D. Li, H. Zhang, Y. Wang, and K. Du, *Opt. Commun.* **229**, 349 (2004).
3. P. Shi, D. Li, H. Zhang, and K. Du, *Acta Opt. Sin.* (in Chinese) **24**, 491 (2004).
4. K. Du, D. Li, H. Zhang, P. Shi, X. Wei, and R. Diart, *Opt. Lett.* **28**, 87 (2003).
5. H. Zhang, P. Shi, D. Li, and K. Du, *Appl. Opt.* **42**, 1681 (2003).
6. P. Shi, "Slab laser with high power and good beam quality" (in Chinese) Ph.D, Shanghai Institute of Optics and Fine Mechanics, Chinese Academy of Sciences, 2004.
7. E. A. Sziklas and A. E. Siegman, *Appl. Opt.* **14**, 1874 (1975).
8. G. Feng, B. Lü, F. Kong, B. Cai, and Y. Huang, *High Power Laser and Particle Beams* (in Chinese) **9**, 69 (1997).